230 and 492 GHz LOW NOISE SIS WAVEGUIDE RECEIVERS EMPLOYING TUNED Nb/AlO_x/Nb TUNNEL JUNCTIONS

J.W. Kooi[1], M. Chan[1], B. Bumble[2],
H.G. LeDuc[2], P.L. Schaffer[1], and T.G. Phillips[1]

1- Caltech Submillimeter Observatory
Division of Physics, Mathematics and Astronomy
California Institute of Technology, Pasadena, California 91125

2- Center for Space Micorelectronics Technology, Jet Propulsion Laboratory

Abstract

We report results on two full height waveguide receivers that cover the 200-290 GHz and 380-510 GHz atmospheric windows. The receivers are part of the facility instrumentation at the Caltech Submillimeter Observatory on Mauna Kea in Hawaii. We have measured receiver noise temperatures in the range of 20K-35K DSB in the 200-290 GHz band, and 65-90K DSB in the 390-510 GHz atmospheric band. In both instances low mixer noise temperatures and very high quantum efficiency have been achieved. Conversion gain (3 dB) is possible with the 230 GHz receiver, however lowest noise and most stable operation is achieved with unity conversion gain.

A 40% operating bandwidth is achieved by using a RF compensated junction mounted in a two-tuner full height waveguide mixer block. The tuned Nb/AlO_x/Nb tunnel junctions incorporate an "end-loaded" tuning stub with two quarter-wave transformer sections to tune out the large junction capacitance. Both 230 and 492 GHz SIS junctions are 0.49μm^2 in size and have current densities of 8 and 10 kA/cm^2 respectively.

Fourier Transform Spectrometer (FTS) measurements of the 230 and 492 GHz tuned junctions show good agreement with the measured heterodyne waveguide response.

Introduction

Two full height waveguide superconductor-insulator-superconductor (SIS) heterodyne receivers with center frequencies of 230 and 492 GHz have been designed and installed at the Caltech Submillimeter Observatory (CSO) on Mauna Kea in Hawaii. The SIS quasiparticle tunnel junction mixer is known to have great potential for producing heterodyne receivers with noise performances approaching the quantum limit [1]. The low noise results discussed here were achieved by employing a 0.49μm^2 Nb/AlO_x/Nb tunnel junction with a lithographically produced "end-loaded" stub matching network to tune out the junction capacitance.

Traditionally, high quality non-contacting backshort and E-plane tuners have been relied upon to tune out the large geometric junction capacitance. This however places a severe demand on the waveguide tuners and results in a relatively small frequency range over which an adequate match to the junction can be achieved [2], (Fig. 2). To improve the junction match to the embedding impedance and increase the instantaneous bandwidth of the mixer a variety of inductive tuning stubs have been introduced [6-14]. The series tuned "end-loaded" stub as discussed in [3, 16-17] has been used in the junction designs because it has several advantages over the conventional open and short circuit shunted stubs. The mixer block incorporates magnetic field concentrators [4]

and a 1-2 GHz wide IF matching network [5].

RF Matching Network

For an SIS tunnel junction the geometric capacitance of the two niobium films separated by a very thin insulator dielectric, ($\approx$ 12 Å), is in parallel with the quantum reactance of the tunnel barrier. For bias voltages on the first quasi-particle step the imaginary part of the junction's RF admittance is nearly zero, and the junction susceptance is dominated by the geometric capacitance, C_j. The RF conductance, $G_j{}^{-1}$ for a junction is described by Tucker's quantum theory. In the low LO power limit where $\alpha \equiv eV_{lo}/\hbar\omega < 1$, G_j is given by the slope of the line joining points on the pumped IV curve one photon step above and below the dc bias point [18]. R_j ranges from $R_n/3$ in the lower part of the sub-millimeter band to $\approx R_n$ for frequencies $\geq$ 500 GHz. R_n is the above gap normal state resistance of the SIS tunnel junction.

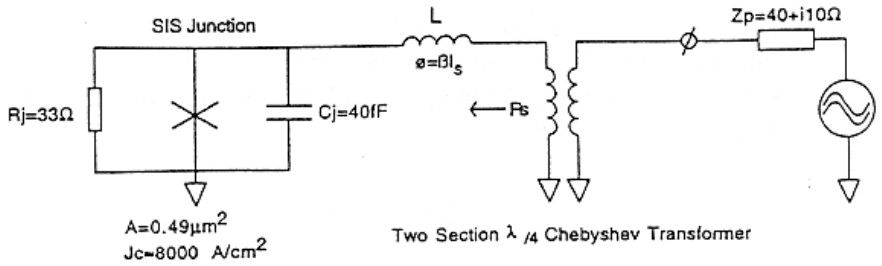

Fig. 1. Electrical diagram of the RF matching network at 345 GHz. The probe impedance is defined as the impedance seen by the bowtie antenna placed in the center of the waveguide.

The admittance of the junction can thus be described as

$$Y_j = (G_j + i\omega C_j) \tag{1}$$

Where C_j is the junction capacitance which can be approximated by

$$C_j \approx (40fF + 4J_c)/\mu m^2 \tag{2}$$

J_c is the current density of the junction in kA/cm^2. The RF conductance varies slowly with frequency and for our design purposes is assumed to be constant. To transform the junction admittance, Y_j, to the embedding impedance presented by the bow-tie antenna probe positioned in the center of the waveguide we used an "end-loaded" stub. The waveguide embedding impedance is a function of frequency and in the ideal case can be adjusted to give a conjugate match to the transformed junction impedance by tuning the E-plane and backshort tuners.

For our design purpose however we have taken it to be constant at 40+10i Ω, which was obtained from scale mixer model measurements.

The "end-loaded" stub puts a small section transmission line in series with the junction. This results in the transformation of the complex junction admittance, Y_j to the real axis on the Smith Chart, R_s. From [3] we see that R_s and βl_s, the electrical length of the "end-loaded" stub, can be approximated as

$$tan(\beta l_s) \simeq 1 - \frac{1}{2K^2} \ , \quad K > 1.2 \tag{3}$$

and

$$R_s \approx \frac{R_j}{2K^2} \approx R_j cos(2\beta l_s) \tag{4}$$

Where $K \equiv \omega R_j C_j$.

As the frequency increases we see from (3) that the stub length l_s approaches $\pi/4$ resulting in very small values of R_s (4). This is a serious drawback of the "end-loaded" stub. For frequencies above 500 GHz it gets more and more difficult to transform R_s to match the probe impedance over a reasonable bandwidth.

To transform R_s to the RF embedding impedance we used a two section equal-ripple Chebyshev transformer [19]. This type of transformer gives the maximum bandwidth while allowing a tolerable pass band ripple. If we define ρ_m as the maximum allowed voltage reflection coefficient of the passband ripple, we can derive the impedances for the two quarter-wave sections that give the widest possible fractional bandwidth.

$$Z_1^2 \approx \frac{R_p}{K}\sqrt{\frac{R_j R_p}{2}}\sqrt{\frac{1-\rho_m}{1+\rho_m}} \ , \quad K \gg 1 \tag{5}$$

$$Z_2^2 \approx \frac{R_j}{4K^3}\sqrt{2R_j R_p}\sqrt{\frac{1+\rho_m}{1-\rho_m}} \ , \quad K \gg 1 \tag{6}$$

Z_1 is the high impedance section which connects to the probe and Z_2 is the low impedance section connected to the "end-loaded" stub (Fig. 3). R_p is the real part of the embedding impedance.

Equations (5) and (6) show that $Z_1 \propto K^{-0.5}$ and $Z_2 \propto K^{-1.5}$. For frequencies in the upper half of the submillimeter band Z_2 becomes very small for junctions with current densities less than 10 kA/cm^2. In practice it is difficult to realize a very low impedance superconducting microstrip transmission line because its aspect ratio, (length/width), becomes rather small. Connecting the high impedance "end-loaded" stub to a low impedance transmission line results in a large discontinuity which increases the effective electrical length of the "end-loaded" stub. This is an especially serious effect at frequencies above 500 GHz considering that the center frequency of the RF matching network is critically dependent on

the "end-loaded" stub's electrical length. Radially shorted inductive stubs [11] and two junction type tuning circuits as described by Zmuidzinas *et al.* [15] are good candidates for the upper half of the submillimeter band.

Junction Design

The 230 and 492 GHz mixer waveguides support single, TE_{10}, mode operation from 150-296 GHz and 316-633 GHz respectively. These along with the newly installed 665 GHz receiver [20] provide complete coverage for the 180-730 GHz CSO submillimeter astronomy band. To achieve a good match over the desired frequency bands it is imperative that a probe impedance, $Z_p(\omega)$, is selected that can easily be tuned to over the entire frequency range [13, 21-22]. Scale model measurements on a full-height waveguide show that the embedding impedance of a probe centered in the guide, with 45 degree lead shapes, is in the order of 35-40 Ω and slightly inductive. In Figure 2 we plot the input impedance of both the 230 GHz and 492 GHz "end-loaded" stub tuned junctions and untuned junctions.

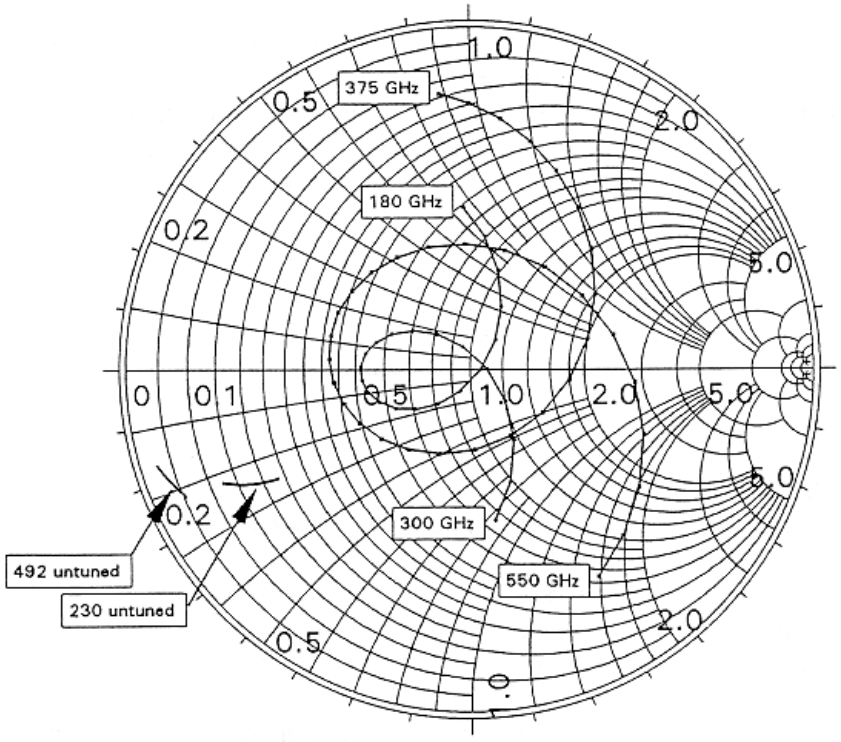

Fig. 2. 230 GHz and 492 GHz tuned and untuned junction impedance plot normalized to 50 Ω. For the untuned junctions very high quality (Q) tuners are needed to tune the probe impedance to Z_j^*.

The maximum voltage reflection coefficient, ρ_m, from 220-280 GHz is -12 dB and -7 dB from 400-500 GHz.

By adjusting the non-contacting tuners we can keep $Z_p\ (\omega)$ approximately constant over the entire frequency range, or tune to a conjugate match. To keep the $\omega R_j C_j$ product (K) as small as possible, allow good coupling to an IF impedance of 160 Ω [5], and maintain high quality junctions we decided to use 50 Ω, 0.49μm^2 Nb/AlO$_x$/Nb SIS tunnel junctions with current densities of 8-10 kA/cm^2. Using Tucker theory, the RF resistance of the pumped IV curve for small values of alpha is approximately .55R_n at 230 GHz and 0.85R_n at 492 GHz.

The "end-loaded" stub length and transformer impedance sections Z_1 and Z_2 were initially calculated using a 40 Ω probe impedance. We then ran Touchstone [24] to optimize the transformer to an embedding impedance of $40+10i\ \Omega$, which in practice did not have much effect. The width's and length's of the optimized normal metal microstrip were used to calculate the characteristic impedance and electrical length of the individual sections using Linecalc [24].

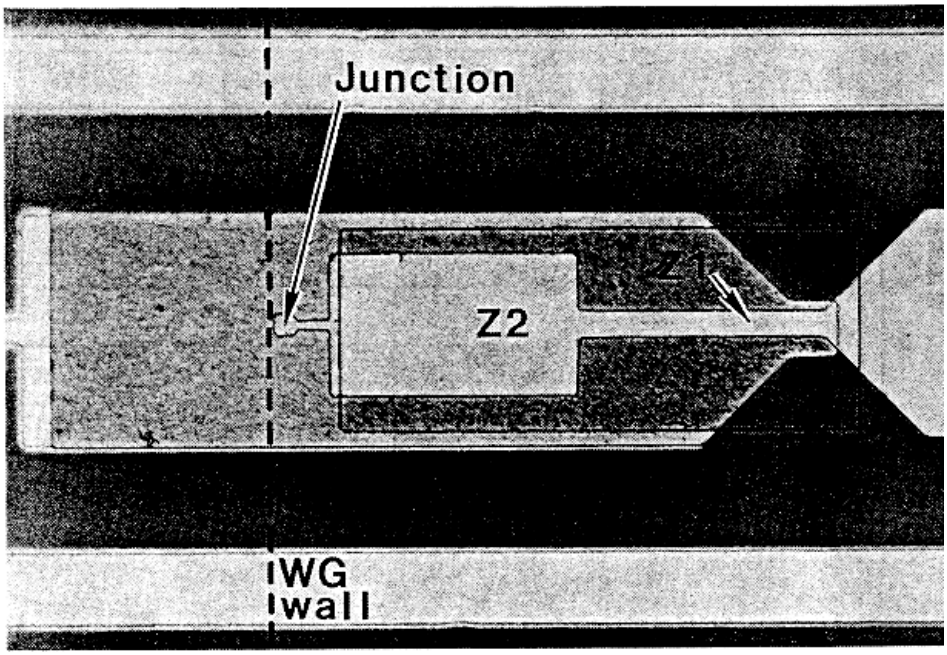

Fig. 3. Physical layout of a 492 GHz tuned junction. The junction and "end-loaded" stub are fabricated on 150nm SiO while the two section transformer is fabricated on 450nm SiO. The junction is deposited

inside a 5 x 5 μm^2 pad whose effect has been taken into account in the computer simulations. Table 1 gives the different junction and transmission line parameters.

Using a program developed by Zmuidzinas *et al.*[25], we proceeded to calculate the required superconducting microstrip width, length and effective dielectric constant of the different line sections. This procedure was iterative because the junction mask was layed out using integer length and width dimensions for different superconducting microstrip transmission line sections. The numerical results of the superconducting transmission line sections are summarized below. Y_o is the characteristic admittance of the end loaded stub transmission line.

Table 1

230 GHz and 492 GHz Tuned Junction Parameters.

	230 Theory	230 Optimized Results	492 Theory	492 Optimized Results
$Z_p{}^*(\Omega)$	$40+0i$	$40-10i$	$40+0i$	$40-10i$
ρ_m	0.2512	0.2445	0.3981	0.3981
$\beta l_s(^\circ)$	38.3	40.2	44.5	39.4
$Y_o\ (\Omega^{-1})$	0.0578	0.0702	0.1236	0.1104
$R_s(\Omega)$	5.28	4.01	0.726	0.827
$Z_1(\Omega)$	20.86	16.41	11.89	11.74
$Z_2(\Omega)$	9.48	6.22	2.39	2.41

To verify the design of the "end-loaded" stub tuning structure we mounted the junctions in a quasi-optical system [16] and ran a series of Fourier Transform Spectrometer (FTS) measurements. To understand the direct detection results we measured the Quasi-optical antenna impedance on a scale model, and used Touchstone to simulate the response (Fig. 4). Also shown in Figure 4 is the theoretical response of the "end-loaded" stub if the embedding impedance were fixed at the design value of 40 Ohms. The measurements show reasonably good agreement with theory as far as the frequency response is concerned. This method has in fact proved to provide quick and accurate information on the overall heterodyne response of the waveguide receivers.

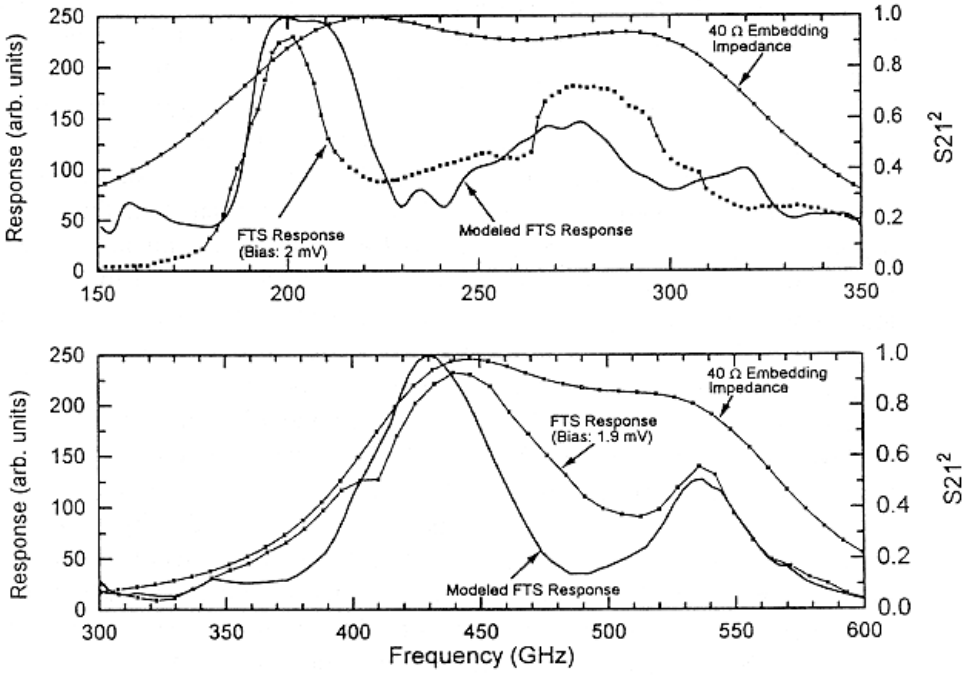

Fig. 4. 230 and 492 GHz FTS measurements. The bowtie antenna and choke structure were mounted at the focus of a quartz hyper-hemispherical lens. Scale model measurements yielded the antenna impedance that was used in the computer simulations.

Receiver Description

Optics

The block diagram of the 230 and 492 GHz receiver is similar to that of the 665 GHz receiver [20]. The optics was designed to give a 14 dB edgetaper on the secondary mirror of the telescope. Local oscillator (LO) injection for the 230 and 492 GHz receivers is accomplished with 5 μm and 19 μm mylar beam splitters mounted at 45° to the LO path. The local oscillator's electric field is perpendicular to the plane of incidence with about 0.12% LO radiation coupled into the cryostat in case of the 230 GHz receiver and 4.3% in the case of the 492 GHz receiver. The remainder is absorbed by a sheet of Eccosorb. The vacuum window for the 230 GHz receiver is made out of 19 μm HR500/2S material manufactured for food packaging by Hercules Inc. [27]. It has a dielectric constant of ≈ 2.6 and is a laminate of biaxially oriented polypropylene with 2.5 μm layers of polyvinlidene chloride on both sides. Laboratory experiments have shown that the material has adequate strength to function as a vacuum window for apertures diameters $\leq$ 25 mm. Experiments indicate that this Hercules material is considerably more opaque to He^4 than 25 μm mylar. Long term operation ($>$ 6 month) of cryostats with the Hercules material in place show much lower permeability to water and atmospheric gasses than 25 μm mylar in a similar period of time. The 492 GHz pressure window consists of a 25mm single crystal quartz disk with a quarter wave teflon anti-reflection coating on both sides[26]. The infrared blocking filter on the 12K window consists of a half wavelength thick fluorogold disk. To help avoid standing waves between the secondary and the instruments, the vacuum windows and IR blocks were tilted at 5 ° angles. The mixer lens is made out of low density polyethelene, with an approximate dielectric constant of 2.41 at 4.2K ambient temperature. To minimize the optical loss of the 12K infrared filter we compared the transmission properties of both fluorogold and fluorosint. Fluorosint is easier to machine than fluorogold, but has a slightly higher dielectric constant. With the receiver tuned to 230 and 434 GHz we obtained the hot (293K) and cold (80K) IF power response with and without an optically thick 'lossy' slab of material inserted in the beam [20, 28]. The reflection corrected transmission loss for fluorogold and fluorosint at 230 and 434 GHz are shown in Table 2.

The optics are designed to give a frequency independent illumination of the secondary (Goldsmith [29]). The low loss polyethylene lens is placed in the near field of a scaler feedhorn. Antenna pattern measurements give reasonably close agreement to the theoretically expected response.

Table 2

230 GHz Measured Absorption Loss

Material	Dielectric Constant (ϵ')	α (np/mm)	tan(δ)
Fluorogold	2.56-2.64	.023	6.0×10^{-3}
Fluorosint	3.55-3.65	.028	6.1×10^{-3}

434 GHz Measured Absorption Loss

Material	Dielectric Constant (ϵ')	α (np/mm)	tan(δ)
Fluorogold	2.56-2.64	.046	6.3×10^{-3}
Fluorosint	3.55-3.65	.056	6.5×10^{-3}

Mixer Block Construction

The full height waveguide mixer blocks are based on the design by Ellison *et al.* [2] and use magnetic field concentrators to suppress the Shapiro step responses [4]. The mixer blocks utilize a double tuning structure and are composed of four sections. The front section constitutes the corrugated feedhorn while the second section holds the circular to rectangular waveguide transformer and E-plane tuner. Four $1/4\lambda_g$ transitions were used to transform the circular TE_{11} mode to the full height TE_{10} mode over the specified frequency range. The E-plane tuner is situated $1/2\lambda_g$ in front of the junction. The third section is the junction block with the built in IF matching network, while the last section holds the non-contacting rectangular backshort tuner. The 230 and 492 GHz junctions are mounted in 200 μm by 200 μm and 100 μm by 100 μm grooves respectively. The groove has been cut across the face of the waveguide parallel to the E-field. The fused quartz substrate dimensions for the 230 junction are 175 μm in width and 100 μm in height and 65μm by 50μm for the 492 junction. Care has been taken to center the bowtie antenna in the waveguide. Silver paint has been used to make contact with both ground and IF side of the RF choke. The IF side of the junction contacts a 25 μm Au wire which is soldered to a 1-2 GHz wide IF

matching network situated in the junction block. The matching network is designed to transform a 160 Ohm IF impedance to 50 Ohms and to provide a short to out of band signals up to $\approx$ 22 GHz. The latter is needed to avoid saturating the junction with unwanted out of band signals. The output of the mixer block is directly connected to a 1-2 GHz 4-5 Kelvin balanced HEMT amplifier, which is based on work by Padin *et al.* [30]. Any impedance mismatch between the matching network and low noise amplifier is absorbed by the amplifier's input Lange coupler (S11 < -12 dB). The RF choke structure consists of a 4 section Chebyshev bandpass filter designed to give a short at the waveguide wall and maximum rejection at the band's center frequency. Rectangular non-contacting tuners are used in the mixer block for both the backshort and E-plane tuners as described by Brewer and Räisänen [31]. All tuners have three low and high impedance sections. To provide a stable voltage bias to the junction we put a 100 Ω resistor in parallel with the junction and a 20 Ω current sense resistor in series with the junction [32, 33].

$180 - 290\,GHz$ *Results and Discussion*

The 276 GHz pumped/unpumped I-V curves and hot(285K)/cold(77K) total power response are shown in Figure 5. The Shapiro steps were carefully suppressed by adjusting the magnetic field. Data was taken "in situ" at the Caltech Submillimeter Observatory in Hawaii.

For SIS mixers operating with a mixer conversion loss > 3 dB it is common to tune for maximum IF power or pumped junction current. Tuning for maximum IF power under these conditions nearly always gives the lowest mixer conversion loss because the IF mismatch is very small and the receiver output noise power is almost completely determined by the mixer conversion loss. The conversion loss was derived from the shot noise method [34], and has been corrected for the IF mismatch between the junction and low noise amplifier. With conversion gains exceeding unity the IF junction impedance is $\gg R_n$, or even negative, which increases the IF mismatch and limits the sensitivity of the receiver. The optimum trade-off between mixer conversion gain and IF coupling efficiency is typically found by first tuning the receiver for maximum IF power at a pumped SIS current of about 1/4 I_c and then optimizing the Y-factor (sensitivity) by adjusting the backshort tuner and/or E-plane tuner. When tuning the receiver in this way one observes a sharp drop in total power (up to 60%), due the decrease in conversion gain, without much affecting the pumped junction current. We found that the best receiver noise temperatures typically correspond to a mixer conversion gain of about unity.

To further understand the breakdown of the measured 22K DSB receiver noise temperature shown in Figure 5, we employed a technique described by Blundell/Feldman *et al.* [35, 36]. By plotting the total IF power as a function

of input load temperature for different values of LO drive level we obtained an equivalent front end receiver noise temperature of 10 ± 2 Kelvin, Shot noise calculated IF contribution of ≈ 5K and quantum limited mixer response.

The receiver response of Figure 5 was optimized for lowest noise temperature (i.e. largest Y-factor) instead of maximum IF noise power. With the existing IF matching scheme, a cooled isolator or balanced IF amplifier is needed to absorb the possibly large reflections between the junction and low noise amplifier.

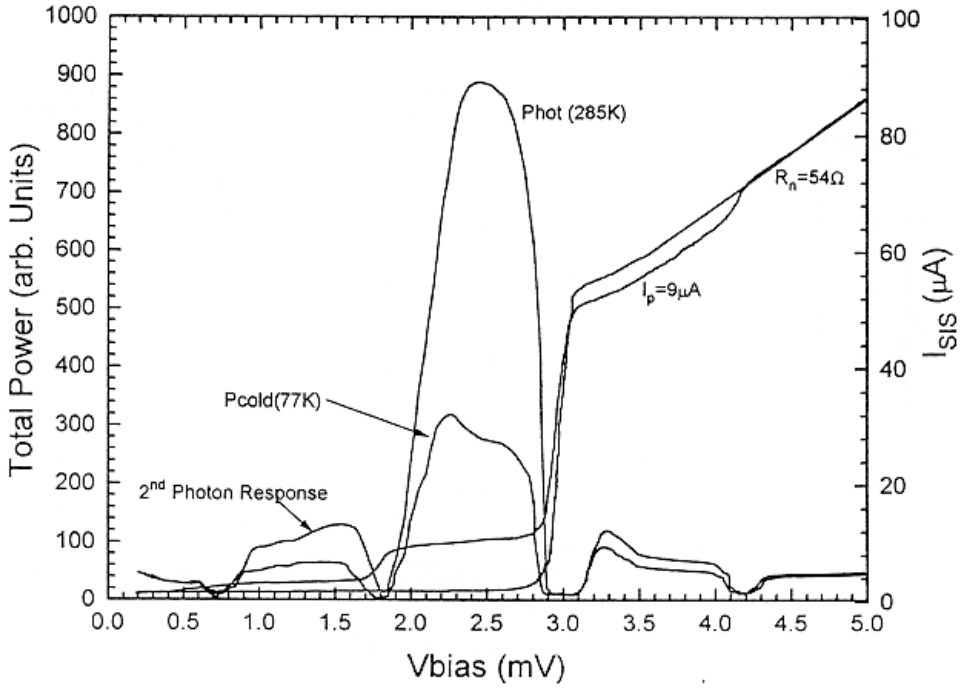

Fig. 5. I-V / Total power response. The optimum receiver noise temperature at 276 GHz was 22 ± 2K DSB with an uncorrected mixer noise temperature of ≈ 18K and 0.5dB of mixer conversion loss. The junction has a resistive subgap to Rn ratio of 32.

Figure 6 depicts the total power and I-V response of the receiver tuned for maximum IF power response at 230 GHz. Note the negative differential resistance on the first photon step below the gap and the unusually strong second photon response. Tuning the receiver in this manner causes several problems. The negative slope of the pumped sub-gap I-V curve allows for reflection gain, which is readily observed on the IF port as oscillations and total IF power instabilities.

This is even the case with the Josephson effect carefully suppressed. In some instances the oscillations were dependent on the load at the mixer input port. A second problem is the intermediate frequency coupling efficiency. The IF matching network is designed to transform a 160 Ohm load to the 50 Ohm low noise amplifier (LNA) input impedance. Presenting the matching network with a negative or very high IF impedance results in large reflections and a poor coupling efficiency to the LNA.

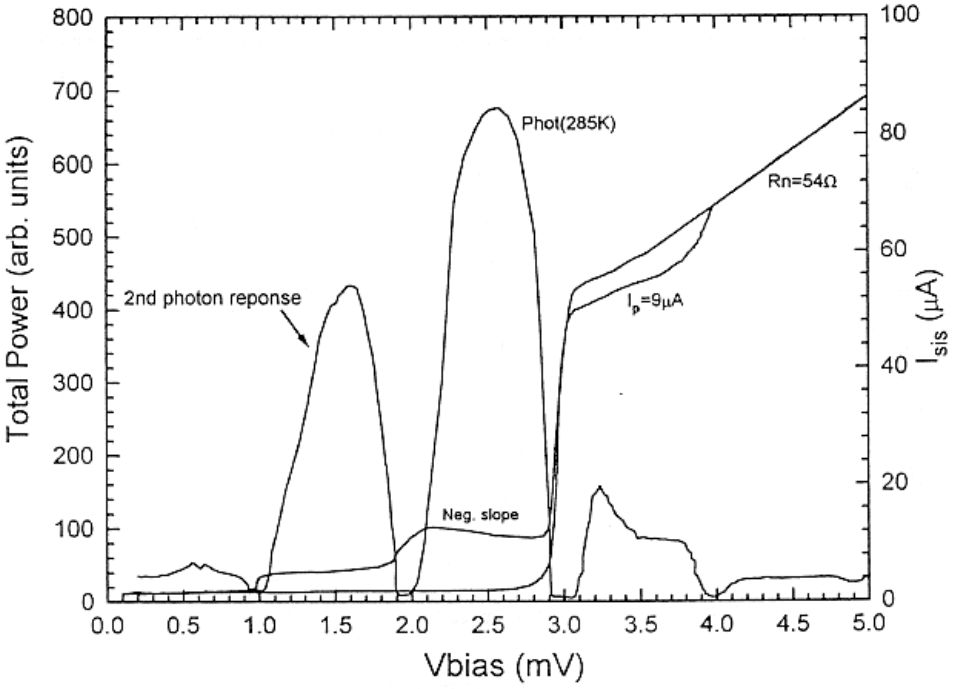

Fig. 6. Hot (285K) total power and I-V response with the receiver tuned for maximum total power at 230 GHz. The receiver has nearly 3dB of conversion gain. Noise temperatures for the 230 GHz receiver tuned in this manner vary from 35-45 Kelvin.

De-tuning the receiver for maximum sensitivity and subsequent unity gain, as described previously, yields a positive differential slope and almost no second photon response (Fig. 5). It turns out that with some experience the 230 GHz receiver can be tuned for optimum sensitivity by forcing a positive pumped I-V curve.

The instantaneous bandwidth for 230 GHz receiver ranges from 4-6 GHz depending on how the receiver is tuned (Fig. 2). This ensures true double

sideband mixer performance for the current 1-2 GHz IF. Figure 8a shows the frequency response of the 230 GHz receiver. It is interesting to note the improvement in receiver noise temperature between the 1991 result with an untuned junction [5] and the discussed tuned junction response. Both receivers use the same LNA, mixer block design and cryostat, the only difference being the junction design. The waveguide overmodes at 296 GHz, which possibly causes the moderate increase in receiver noise temperature.

$380 - 510\,GHz$ *Results and Discussion*

The 492 GHz pumped/unpumped I-V curves and hot(285K)/cold(77K) total power response taken at the CSO are shown in Figure 7. The Shapiro step responses were suppressed as low as possible by adjusting the magnetic field.

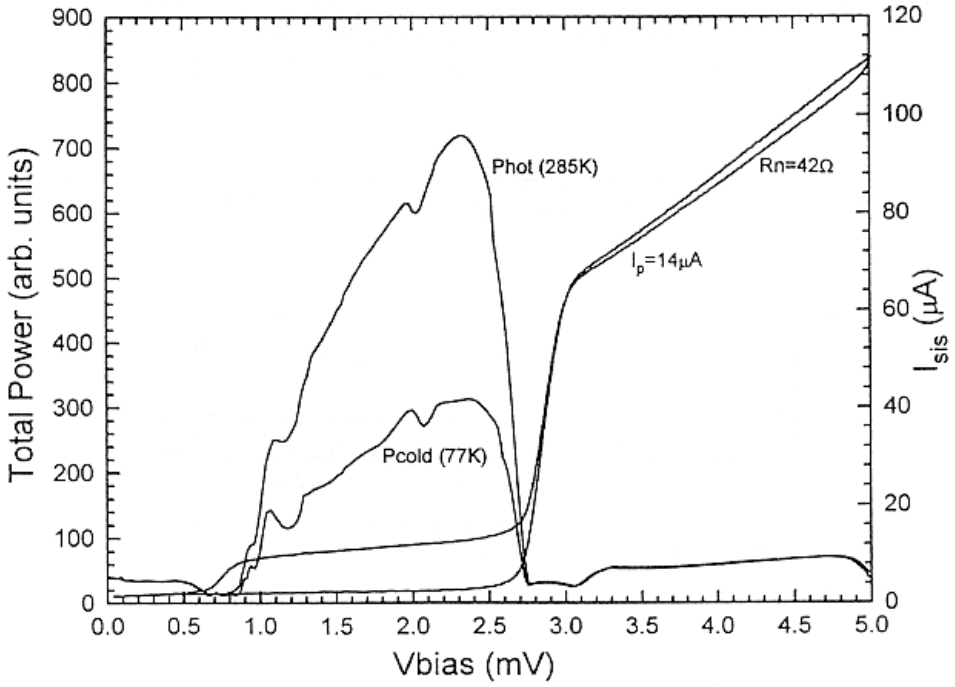

Fig. 7. 492 GHz I-V / Total power response. The optimum receiver noise temperature was 74K ± 2K DSB with an uncorrected mixer noise temperature of ≈ 60K and 3dB of mixer conversion loss. The junction has a Rsg/Rn ratio of 28.

The 230 GHz receiver tuning method applies to some extent to this receiver as well. With the receiver tuned for maximum total power, the slope of the pumped I-V curve is nearly zero indicating that the junction capacitance is effectively tuned out. The IF coupling efficiency in this case is quite poor however, which is readily observed by the IF passband ripple. De-tuning the receiver to get a positive sloped I-V curve and subsequent finite IF impedance improves the receiver noise temperature by as much as 15% (Fig. 7).

Using the Blundell/Feldman method [35, 36] the calculated mixer RF and optics loss is approximately 52 $\pm$ 2K. With a shot noise calculated IF noise contribution of $\approx$ 10K we again observe quantum limited mixer response. It is clear that the receiver noise temperature is limited by the combined optics loss of the beamsplitter, 300K pressure window, 12K infrared blocking filter and 4K focusing lens.

The frequency response of the 492 GHz receiver is shown in Figure 8b. Due to local oscillator availability the receiver noise temperatures from 390-440 GHz were taken in the lab, while data from 444-500 GHz were taken at the CSO.

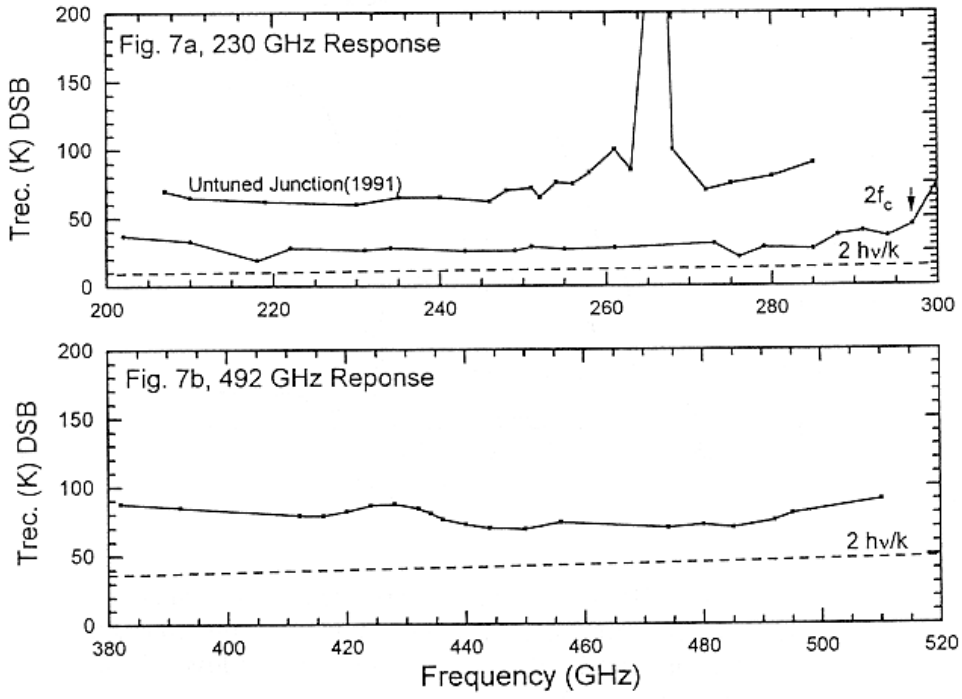

Fig. 8a, b. Frequency response of the 230 and 492 GHz receivers

discussed. Both waveguide receivers employ RF tuned junctions as well as two mechanical tuners. The 1991 data represents achievable receiver noise temperatures without the aid of a RF matching network to tune out the junction capacitance.

The 492 GHz junction has a current density of 10k A/cm^2 with an normal state resistance of 44 Ohm. Tuning the receiver for maximum total power, we measured a DSB noise temperature of 90K and calculate $\approx$ 1 dB of mixer conversion loss. Although it is not ideal, one can in principal operate in this mode. The measured instantaneous bandwidth of the 492 GHz receiver depends on the tuner setting (Fig. 2), but is in general > 15 GHz.

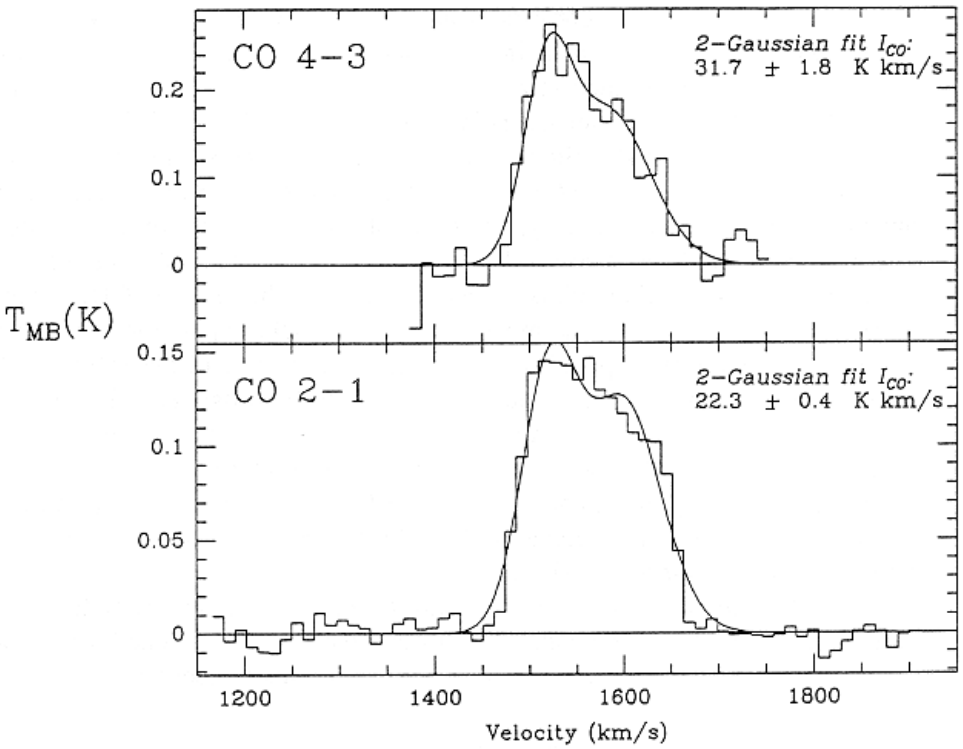

Fig. 9. A spectrum of M100 (NGC 4321) in ^{12}CO $J = 4 \rightarrow 3$ and $2 \rightarrow 1$ taken at the Caltech Submillimeter Observatory. Total integration are 1500 and 300 seconds respectively.

A spectrum of M100 (NGC 4321) in ^{12}CO $J = 4 \rightarrow 3$ and $2 \rightarrow 1$ is shown in Figure 9. At the velocity of this galaxy ($\sim$1550 km/s), this corresponds to central frequencies of 458.7 and 229.3 GHz, respectively. System temperatures and approximate zenith atmospheric transmissions were $\sim$2000K (0.04) at the $4 \rightarrow 3$ frequency and $\sim$200K (0.95) at the $2 \rightarrow 1$ frequency. Both spectra are

corrected for atmospheric attenuation and antenna efficiency, yielding a main beam temperature. The high flux ratio (I_{CO} $4 \rightarrow 3/I_{CO}$ $2 \rightarrow 1$) indicates the presence of large amounts of warm molecular gas. M100 is one of the best-studied spiral galaxies, and the ability to detect the higher J transitions of CO from such objects opens new possibilities in the study of extragalactic sources.

Conclusion

Two SIS heterodyne quasi-particle mixers have been developed for the 180-290 GHz and 380-510 GHz submillimeter bands. The mixers employ tuned 0.49 μm^2 Nb/AlO$_x$/Nb tunnel junctions mounted in full height waveguide blocks. The RF matching network consists of an "end-loaded" stub with a two section equal-ripple transformer, which in combination with a two-tuner mixer block provides for quantum limited mixer response as well as a 40% operating bandwidth. The 230 GHz receiver has noise temperatures below 30K DSB for most of the 200-290 GHz band while the 492 GHz receiver's noise is better than 80K DSB for most of the 380-510 GHz band. Both mixers appear to be substantially quantum noise limited over large fractions of the respective frequency bands. The receivers have been successfully installed at the Caltech Submillimeter Observatory in Hawaii. Although is it very easy to tune the 180-290 GHz receiver to exhibit conversion gain, the most sensitive and stable operation is generally achieved with the mixer operating at unity gain. In the case of the 380-510 GHz receiver, mixer conversion gain does not appear to be possible. It is very easy however to tune out the junction capacitance, and thereby obtain a near infinite IF port impedance with associated problems. The correct tuning procedure for maximum sensitivity and stability is to tune for maximum total IF power, i.e. conversion gain, and then detune the backshort or E-plane tuner a bit to obtain a finite positive pumped I-V slope.

The "end-loaded" stub is a promising technology for the lower frequency half of the submillimeter band. It enables development of tuned waveguide mixers with high quantum efficiency as well as fix-tuned receivers.

Acknowledgments

We wish to thank Jonas Zmuidzinas, Rob Schoelkopf and John Cortese for technical discussions, Dave Miller for help with the optics, Chris Walker for lending us one of his 492 GHz mixer blocks, Dominic Benford and Todd Hunter for the astronomical data, Dave Woody for discussing the IF/Shot noise contribution, Mei Bin for all her work on the FTS and Kooi thanks his wife for her faithful support. Work at Caltech is supported in part by NSF grant# AST 93-13929 and NASA grant# NAGW-107.

References

[1] J.R. Tucker and M.J. Feldman, "Quantum Detection at Millimeter Wavelength," *Rev. Mod. Phys.* 57, 1055-1113, 1985

[2] B.N. Ellison and R.E. Miller, "A Low Noise 230 GHz SIS Receiver," *Int. J. IR and MM Waves*, Vol 8, 609-625, 1987

[3] J. W. Kooi, M. Chan, B. Bumble, T. G. Phillips, "A low noise 345 GHz waveguide receiver employing a tuned 0.50 μm^2 Nb/AlO_x/Nb tunnel junction," *Int. J. IR and MM Waves*, Vol. 15, No. 5, May 1994.

[4] C.K. Walker, J.W. Kooi, M. Chan, H.G. Leduc, P.L. Schaffer, J.E. Carlstrom, and T.G. Phillips, "A Low-noise 492 GHz SIS waveguide receiver," *Int. J. IR and MM Waves*, Vol. 13, pp. 785-798, June 1992.

[5] J.W. Kooi, M. Chan, T.G. Phillips, B. Bumble, and H.G. Leduc, "A low noise 230 GHz heterodyne receiver employing 0.25 μm^2 area Nb/AlO_x/Nb tunnel junctions," *IEEE trans. Microwaves Theory and Techniques*, Vol. 40, pp. 812-815, May 1992.

[6] L.R. D'addario, "An SIS Mixer for 90-120 GHz with Gain and Wide bandwidth," *Int. J. IR and MM Waves*, Vol 5, No. 11, pp. 1419-1433, 1984.

[7] A.V. Räisänen, W.R. McGrath, P.L. Richards, and F.L. Lloyd, "Broad-band RF match to a Millimeter-Wave SIS Quasi-Particle Mixer," *IEEE Trans. Microwave Theory and Techniques,* Vol. MTT-33, No. 12, pp. 1495-1499, 1985.

[8] A. R. Kerr, S.K. Pan, M.J. Feldman, "Integrated Tuning for SIS Mixers," *Int. J. IR and MM Waves*, Vol 9, No. 2, pp. 203-212, 1988.

[9] C.E. Honingh, G. de Lange, M.M.T.M. Dierichs, H.H. Schaeffer, Th. de Graauw, and T.M. Klapwijk, "Performance of a Two-Junction Array SIS-Mixer Operating Around 345 GHz," *IEEE Trans. Microwave Theory and Techniques,* Vol. MTT-41, No. 4, pp. 616-623, 1993.

[10] G. de Lange, C.E. Honingh, M.M.T.M. Dierichs, H.H.A. Schaeffer, H. Kuipers, R.A. Panhuyzen, T.M. Klapwijk, H. van de Stadt, M.W.M. de Graauw, and E. Armandillo, "Quantum limited responsivity of a Nb/Al_2O_3/Nb SIS waveguide mixer at 460 GHz", Proc. 4^{th} Int'l Symp. Space THz Technology, Los Angeles, pp. 41-49, 1993

[11] M. Salez, P. Febvre, W.R. McGrath, B. Bumble, H.G. LeDuc, "An SIS Waveguide Heterodyne Receiver for 600 GHz - 635 GHz," *Int. J. IR and MM Waves*, Vol 15, No. 2, Feb. 1994.

[12] J.W. Kooi, M.S. Chan, M. Bin, B. Bumble, H.G. Leduc, C.K. Walker, and T.G. Phillips, "The Development of an 850 GHz Waveguide Receiver using Tuned SIS Junctions on 1μm Si_3N_4 Membranes," *Int. J. IR and MM Waves*, V16 (2), pp 349-362, Feb. 1995

[13] R. Blundell, C.-Y E. Tong, D.C Papa, R.L. Leombruno, X. Zhang, S. Paine, J.A. Stern, H.G. LeDuc, and B. Bumble, "A wideband fixed-tuned SIS receiver for 200 GHz Operation," *IEEE Trans. Microwave Theory and Techniques,* Vol. MTT-43, April 95, pp.933-937, 1995.

[14] R. Blundell, C.-Y E. Tong, J.W. Barrett, J. Kawamura, R.L. Leombruno, S. Paine, D.C Papa, X. Zhang, J.A. Stern, H.G. LeDuc, and B. Bumble, "A fixed-tuned SIS receiver for 250 GHz frequency band." *Int. J. IR and MM Waves*, Sixth International Symposium on Space Terahertz technology, Pasadena, Ca., March (1995).

[15] J. Zmuidzinas, H.G. Leduc, J.A. Stern, and S.R. Cypher, "Two-junction tuning circuits for submillimeter SIS mixers," *IEEE Transcations on Microwave Theory and Techniques,* Vol. MTT-42, No. 4, pp 698-706, Apr 1994.

[16] T.H. Büttgenbach, H.G. LeDuc, P.D. Maker, T.G. Phillips, "A Fixed Tuned Broadband Matching Structure for SIS Receivers," *IEEE Trans. Applied Supercond.*, Vol. 2, No. 3, pp. 165-175, 1992.

[17] K. Jacobs, U. Kotthaus, and B. Vowinkel, "Simulated Performance and Model Measurements of an SIS Waveguide Mixer using Integrated Tuning Structures," *Int. J. IR and MM Waves*, Vol 13, No. 1, pp. 15-26, 1992.

[18] E.C. Sutton, "A Superconducting Tunnel Junction Receiver for 230 GHz," *IEEE Trans. Microwave Theory and Techniques,* Vol. MTT-31, No. 7, pp. 589-592, 1983.

[19] "Foundations for Microwave Engineering," McGraw-Hill Physical and Quantum Electronics Series. 1966.

[20] J.W. Kooi, C.K. Walker, H.G. LeDuc, T.R. Hunter, D.J. Benford, and T.G. Phillips, "A Low Noise 665 GHz SIS Quasi-Particle Waveguide Receiver," *Int. J. IR and MM Waves*, Vol 15, no 3, pp477-4992, March 1994.

[21] T.H. Büttgenbach, T.D Groesbeck, and B.N. Ellison, "A Scale Mixer Model for SIS Waveguide Receivers," *Int. J. IR and MM Waves*, Vol 11, no 1, 1990.

[22] A.V. Räisänen, W.R. McGrath, D.G. Crete, and P.L. Richards, "Scale Model Measurements of Embedding Impedances for SIS Waveguide Mixers," *Int. J. IR and MM Waves*, Vol 6, No. 12, pp. 1169-1189, 1985.

[23] C.E. Honingh,"A Quantum Mixer at 350 GHz based on Superconducting-Insulator-Superconducting (SIS) Junctions," PhD Dissertation, Groningen, The Netherlands, June 1993.

[24] HP/EESOF CAD, Westlake Village, Ca. 91362.

[25] J. Zmuidzinas, and H.G. LeDuc, "Quasi-Optical Slot Antenna SIS Mixers," *IEEE Trans. Microwave Theory and Techniques,* Vol. MTT-40, No. 9, pp. 1797-1804, September 1992.

[26] Thermech Engineering, 1773 W. Lincoln Ave., Anaheim, Ca. 92801